Journal of Porous Materials (2018) 25:1603–1609
https://doi.org/10.1007/s10934-018-0574-7

Synthesis of a highly hydrophobic silica mesostructure by a modified co-condensation procedure and evaluation of its drug release capability

Marcela Bloise Costa[1] · **Marcos Augusto Bizeto**[1]

Published online: 6 February 2018

Abstract
A highly hydrophobic silica mesostructure was synthesized by a modification on the conventional co-condensation procedure that involved the partial substitution of hexadecyltrimethylammonium, used as mesostructure directing agent, by hexadecyltrimethoxysilane. That modification allowed the production of a highly ordered hexagonal silica mesostructure with the mesopores partially filled with high amounts of hexadecyl chains, covalently bonded to inorganic framework. After extracting the reminiscent template molecules, ibuprofen was loaded into the mesostructure in order to evaluate its drug release properties. The drug loading amount (21 wt%) was comparable to the one reported for MCM-41 with grafted propylamine groups (25 wt%), indicating that C_{16}-chains were not fully compacted occluding the pores. A slow ibuprofen release was observed in simulated body fluid (pH 7.2) by a process controlled by an anomalous transport with contribution of diffusional and relaxational components, according to the Korsmeyer-Peppas kinetics model. That hydrophobic mesostructure produced has the potential of being use as a carrier for low water soluble drugs with an extended delivery effect, but without the disadvantages of co-releasing toxic surfactant molecules or the need of non-toxic specific templates to be prepared.

Keywords Hexadecyltrimethoxysilane functionalization · Hydrophobic mesoporous silica · Drug delivery · Molecular nanocontainer · Ibuprofen release

1 Introduction

Mesoporous silicas have an extensive network of nanometric structural pores, whose size and shape are precisely controlled by synthesis [1], conferring to the solid an enormous surface area combined to a large free volume of open pores. These structural characteristics enable the incorporation inside these mesostructures significant amounts of species of different chemical natures, transforming them into molecular nanocontainers that are useful for drug delivery systems [2, 3], pollutant adsorbents [4–6] and supports for catalysts [7–9].

Improvements on the properties of these nanocontainers can be achieved by carrying out chemical modifications on the silica mesostructure, basically using organosilanes that contains functional groups, which permit modulate the established interactions between the inorganic framework and the immobilized molecules [10]. Different alkylsilanes were already used in the chemical modification of mesoporous silicas and the direct synthesis by co-condensation or the post-grafting are the main synthetic strategies to generate these organo-functionalized silicas [11, 12]. Co-condensation is normally preferred over the post-functionalization due to the better distribution of functional groups along the pores [13]. However, this procedure has the disadvantage of only being possible to be carried out with limited amounts (ca. 10 mol%) of organosilane substituting the inorganic source precursor. Otherwise, disordered or collapsed silica mesostructures are produced [14]. Post-grafting methods have the advantage of producing more stable mesostructures but with the disadvantages of concentrating more

Electronic supplementary material The online version of this article (https://doi.org/10.1007/s10934-018-0574-7) contains supplementary material, which is available to authorized users.

✉ Marcos Augusto Bizeto
mabizeto@unifesp.br

[1] Laboratório de Materiais Híbridos, Departamento de Química, Instituto de Ciências Ambientais, Químicas e Farmacêuticas, Universidade Federal de São Paulo, Rua São Nicolau, 210, Diadema, SP CEP: 09913-030, Brazil

functional groups at pores entrance and causing a decrease on the available pore size [12, 13].

The present paper reports a modification in the co-condensation synthetic method that allowed the obtaining of a highly ordered hexagonal hydrophobic silica mesostructure (C_{16}MCM-41) containing high amounts of long pendant hexadecyl chains (C_{16}-chains) covalently bonded to the pore framework. Highly hydrophobic mesoporous silicas containing grafted C_{16}-chains [15, 16] have already been investigated on the production of pickering water-in-oil emulsion droplets for colloidosome preparation [17], to isolate fatty acids from microalgae oil [18], to adsorb 4-nonylphenol through a cooperative process with aminoproyl groups [19], to adsorb organic pollutants from water [15] and to immobilize and stabilize enzymes for catalytic processes [20].

Hydrophobic interactions can be used to modulate the kinetics of drug release in mesoporous silicas, as already reported for ibuprofen [± 2-(*p*-isobutylphenilpropanoic acid)] release from mesoporous silicas post-grafted with small alkylic chains [21–23] or to silica mesophases (containing hexadecylammonium template molecules filling the pores) in the delivering of nutraceuticals molecules [24]. Silica mesophases are easy to prepare, but surfactants such as hexadecyltrimethylammonium are high toxic [25] and cannot be released from the mesophase. Thus the effectiveness of this approach depends on using specific non-toxic structural directing agents [26, 27] or to covalently bond the alkylic chain to the silica framework, as described in this paper.

The loading and releasing of ibuprofen from this hydrophobic nanocontainer were also investigated and the results demonstrated the potential of this mesostructure as a carrier for low water soluble drugs with extended delivery capability.

2 Experimental procedures

2.1 Chemicals

Tetraethylorthosilicate (TEOS, Aldrich), concentrated ammonium hydroxide solution (NH_4OH 30 wt%, Synth), hexadecyltrimethylammonium bromide (HDTMAB, Aldrich), hexadecyltrimethoxysilane (HDTMS, Aldrich) and ibuprofen (Ibu - PharPlus) were used as received. Hexane (Synth), ethanol (Synth), concentrate HCl (Synth) and deionized water (H_2O DI) were used without prior purification. Simulated body fluid (SBF) for drug release assays was prepared by mixing specific amounts of NaCl (Synth), $NaHCO_3$ (Synth), KCl (Synth), $K_2HPO_4{\cdot}3H_2O$ (Synth), $MgCl_2{\cdot}6H_2O$ (Synth), $CaCl_2$ (Synth), Na_2SO_4 (Synth), $(HOCH_2)_3CNH_2$ (Tris-Aldrich) and HCl in H_2O DI according to the recipe published elsewhere [28].

2.2 Synthesis of C_{16}MCM-41 mesostructure

C_{16}MCM-41 was synthesized by a modified co-condensation method, where a mixture of TEOS and HDTMS were hydrolyzed in a NH_4OH aqueous solution of HDTMAB micellar aggregates. In the conventional co-condensation method, a small portion of the silica source is substituted by the organosilane, maintaining constant the silicon molar amount. In this modified procedure the amount of the silica precursor (TEOS) was not altered, but half of the molar amount of the HDTMAB required to produce the MCM-41 phase was replaced by HDTMS. Overall reactants molar ratios were 525(H_2O):69(NH_4OH):0.0625(HDTMAB):0.0625(HDTMS):1(TEOS).

First HDTMAB was dissolved in NH_4OH aqueous solution and then the mixture of TEOS and HDTMS was slowly added to the solution under continuous stirring at room temperature. After 2 h of reaction a white solid was isolated by filtration, washed with copious portions of water DI and dried at 100 °C. This solid will be referred hereafter in the text as HDTMA@C_{16}MCM-41 and it was characterized by powder X-ray diffractometry (PXRD), thermogravimetric analysis (TGA) and Fourier transform vibrational spectroscopy at infrared region (FTIR). Chemical composition was determined by C H N elemental analysis and textural properties determined by registering the N_2 adsorption and desorption isotherms (N_2ADI).

Template removal was carried out by solvent extraction using a mixture of concentrate HCl in ethanol at a 1:4 volume proportion. 1 g of the as-synthesized solid was suspended in 20 mL of that extraction solution, where remained at constant stirring for 24 h. This procedure was twice repeated in order to guarantee the complete $HDTMA^+$ removal. Then the solid was washed with DI water till the washing solution reached a pH value around neutral. The solid obtained in this step will be referred hereafter in the text as C_{16}MCM-41 and it was characterized by PXRD, TGA and FTIR. Chemical composition was determined by C H N elemental analysis and textural properties determined by N_2ADI.

2.3 Ibuprofen immobilization and drug release assay

Ibuprofen loading into C_{16}MCM-41 was performed suspending 500 mg of the dried mesostructure in 20 mL of a 0.26 $mol{\cdot}L^{-1}$ drug solution in hexane for 5 days at room temperature. After this period, the solid was isolated by filtration, washed with hexane to remove residual non-adsorbed ibuprofen molecules and then dried at 50 °C in a vacuum oven for 24 h. This solid will be referred hereafter

in the text as Ibu@C_{16}MCM-41 and it was characterized by PXRD, TGA and FTIR. Chemical composition was determined by C H N elemental analysis.

Drug release assays were performed in triplicate using 13 mm pellets produced by pressing 100 mg of Ibu@C_{16}MCM-41 in evacuable pellet press at 80 kN for 10 min. Pellets were placed in a closed vial adapted with a magnetic stirring bar holder (to avoid the direct contact with pellets), then 20 mL of SBF was introduced in the vial and the solution was gentle stirred at 37 °C. After determined time intervals the solution in the vial was fully drained and the absorbance at 263 nm was registered in order to evaluate the amount of ibuprofen released using the Beer–Lambert law. The vial was refilled with a fresh 20 mL portion of SBF and the process repeated during the time intervals necessary to determine the cumulative ibuprofen release over 400 min.

2.4 Samples characterizations

X-ray diffraction patterns of powdered samples were recorded on a Rigaku Miniflex diffractometer using Cu(K_α) radiation. Thermogravimetric analyses were recorded on a Netzsch thermoanalyser model TGA/DSC 490 PC Luxx, using alumina crucibles, synthetic air atmosphere (50 mL·min^{-1} of flow) and a heating rate of 10 °C·min^{-1}. Fourier transformed infrared spectra of solid samples diluted in KBr were recorded on a Shimadzu spectrophotometer, model IRPrestige 21 using the DRIFT accessory, 4 cm^{-1} of resolution and 64 scans. UV–Vis electronic absorption spectra were recorded in UV range in an OceanOptics spectrophotometer, model USB4000 equipped with deuterium/halogen lamps. C H N elemental analyses were recorded on Perkin Elmer 2400 series II equipment. N_2 adsorption/desorption isotherms of degassed samples at 80 °C and reduce pressure were registered at 77 K on an ASAP 2020N Automatic Physisorption Analyzer from Micromeritics.

3 Results and discussions

3.1 Materials characterization

As both HDTMAB and HDTMS have the same C_{16}-chains, the initial attempt was to try to synthesize the mesostructure without $HDTMA^+$, using only the HDTMS as structure directing agent. This was not effective, since the solid product was not formed in suitable yields, which impaired its isolation. Furthermore, its PXRD analysis indicated the formation of an amorphous mesophase without long range mesostructural ordering. On the other hand, when the synthesis was made using HDTMAB:HDTMS at a molar ratio of 1:1, a highly ordered hexagonal mesostructure with the same symmetry expected to MCM-41 was produced. PXRD

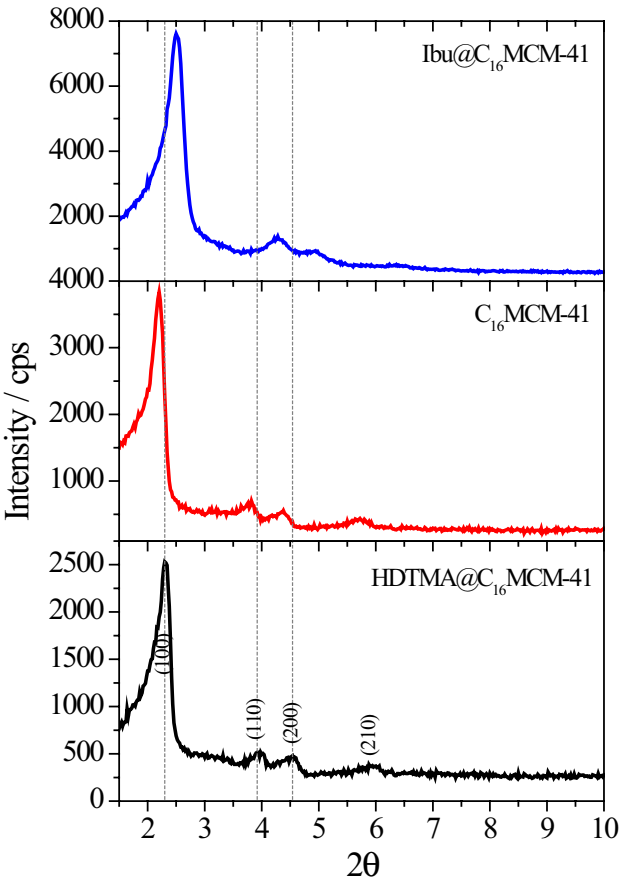

Fig. 1 PXRD of as-synthesized silica (HDTMA@C_{16}MCM-41), after template removal (C_{16}MCM-41) and with ibuprofen immobilized by adsorption (Ibu@C_{16}MCM-41). Dashed grid lines were used in order to facilitate the visualization of diffraction peaks shifts in relation to the peaks of as-synthesized silica

pattern of HDTMA@C_{16}MCM-41 (Fig. 1) presented four diffraction peaks attributed to the p6mm (bidimensional) hexagonal space group. The calculated a_0 unit cell parameter of 44.8 ± 0.3 Å was compatible to the expected value of mesophases constructed using only $HDTMA^+$ micellar aggregates as structure directing agent [29]. The calculated a_0 values from each one of the diffraction peaks were very close, indicating the formation of a regular hexagonal mesostructure with long range ordering (see Table S1 in Electronic Supplementary Material). Contrarily, by using the conventional co-condensation procedure, where 10 mol% of TEOS was replaced by HDTMS, the formation of a cubic Ia3d structure was reported [16].

After $HDTMA^+$ extraction, the calculated a_0 unit cell parameter of C_{16}MCM-41 was 46.3 ± 0.1 Å, which represents a pseudo structural enlargement in relation to the as-synthesize mesophase. Actually, this structural enlargement is related to a phenomenon of electronic contrast increasing between the inorganic silica walls and the partial filled pores

due to $HDTMA^+$ extraction [30]. The hexagonal ordering of the mesostructure was not affected after template removal.

After ibuprofen loading into C_{16}MCM-41, the a_0 unit cell parameter decreased to 41.1 ± 0.3 Å possibly due to the filling of void spaces between the C_{16}-chains inside the pores. Diffraction peaks related to crystalline phases of ibuprofen were not observed [31] (see Figure S1 in Electronic Supplementary Material), which indicates the drug presence as isolated molecules or dimers within the pores, as will be discussed in FTIR analysis. According to NMR studies [32], ibuprofen crystallization into small pore silicas, such as MCM-41, is only possible of occurring at the external surface of particles and do not inside pores due to steric hindrances.

Nitrogen adsorption/desorption isotherms of the mesostructures registered before and after $HDTMA^+$ removal (see Figure S2 in Electronic Supplementary Material) showed type II isotherms with a H3 loop hysteresis that were characteristic of non porous solids [33]. BET method for surface area assessment was not applicable to HDTMA@C_{16}MCM-41 considering the isotherm type and the negative value of the BET constant C (−20.7) [34]. In opposite, for C_{16}MCM-41 the value of C constant was +62.9, but due to the impossibility on separating the processes of N_2 monolayer adsorption and micropores filling in Type II isotherms, the BET surface area of 1.3 $m^2\ g^{-1}$, which should be regarded to the effective area available for the drug adsorption [34], seems to be too inaccurate. Thus, porosity data confirmed the presence of the C_{16}-chains inside the pores of mesostructure but without presenting a reliable evidence of surface area available to drug adsorption.

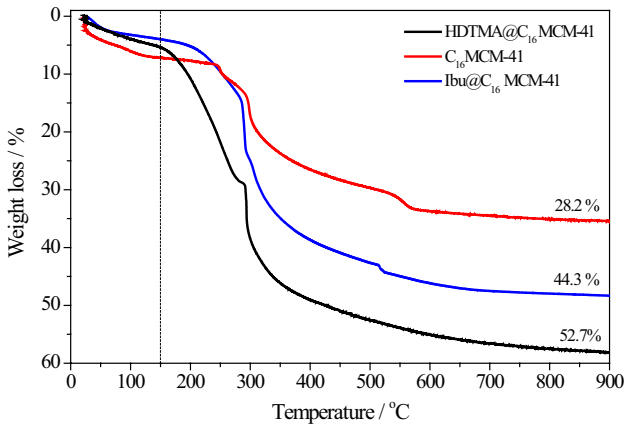

Fig. 2 TGA of as-synthesized silica (HDTMA@C_{16}MCM-41), after template removal (C_{16}MCM-41) and after ibuprofen loading (Ibu@C_{16}MCM-41). Dashed line indicates the temperature limit from which the thermal decomposition of organics began

Changes in chemical composition after $HDTMA^+$ removal and ibuprofen loading were accompanied by TGA and C H N elemental analysis. In TGA curves (Fig. 2) the first weight loss event observed, from room temperature till 150 °C, was attributed to the elimination of adsorbed water molecules in HDTMA@C_{16}MCM-41 and in C_{16}MCM-41 and to the evaporation of residual hexane in Ibu@C_{16}MCM-41. Above this temperature, the weight loss events were related to the thermal decomposition of organic moieties. TGA results were overestimated in comparison to the elemental analysis data because of the elimination of water molecules generated from the condensation reaction between structural silanol groups that occurs above 250 °C [35].

TGA curve of HDTMA@C_{16}MCM-41 indicated the presence of 52.7% of organics. After the template removal, the organics decreased to 28.2% (Fig. 2). According to C H N elemental analysis (Table 1) and considering anhydrous samples, the chemical composition of these compounds were respectively $(C_{19}H_{49}N)_{0.1}(C_{16}H_{33})_{0.09}SiO_2$ and $(C_{16}H_{33})_{0.08}SiO_2$. C H N elemental analysis of C_{16}MCM-41 (Table 1) confirmed the complete extraction of the surfactant molecules, since nitrogen atoms were not detected in that sample. HDTMS and $HDTMA^+$ were incorporated into mesophase at the same molar ratio present in synthetic mixture. The amount of C_{16}-chains grafted into silica framework after template removal was almost 60 times higher than the obtained by the conventional co-condensation method [16] and around 110 times higher than the one obtained by post-grafting [18].

Organics increased to 44.3% after ibuprofen loading (Fig. 2), which corresponds to about 21 wt% of drug loading (1.7 $mmol{\cdot}g^{-1}$ of MCM-41). The determined chemical composition based on C H N elemental analysis was $(C_{13}H_{18}O_2)_{0.1}(C_{16}H_{33})_{0.085}SiO_2$. The ibuprofen loading into C_{16}MCM-41 was lower than the one reported to MCM-41 (ca. 33 wt%) [31, 36], but it was comparable to the amount loaded into propylamine grafted MCM-41 (ca. 25 wt%) [37].

Packaging arrangement of C_{16}-chains inside the mesopores were investigated by FTIR, since the energy of the stretching and bending vibrational modes of C–H bond

Table 1 Proposed chemical composition of prepared mesostructures according to C H N elemental analysis

Sample	C (%)	H (%)	N (%)	Proposed formula
HDTMA@C_{16}MCM-41	37.3	7.5	1.3	$(C_{19}H_{49}N)_{0.1}(C_{16}H_{33})_{0.09}SiO_2$
C_{16}MCM-41	19.8	4.5	0.1	$(C_{16}H_{33})_{0.08}SiO_2$
Ibu@C_{16}MCM-41	32.9	6.0	nd	$(C_{13}H_{18}O_2)_{0.1}(C_{16}H_{33})_{0.085}SiO_2$

nd not detected

in methylene ($–CH_2$) and methyl ($–CH_3$) groups of long alkylic chains are sensitive to the *gauche*/*trans* conformers ratio [38, 39]. By increasing the *gauche* conformer, a shift to higher frequencies of methylene symmetric and asymmetric C–H stretching vibrations are observed [40, 41]. In Fig. 3a, the bands at 2924 and 2854 cm^{-1} of HDTMA@C_{16}MCM-41 were respectively attributed to the C–H asymmetric and symmetric stretching modes of the methylene groups of the C_{16}-chains. C–H vibrational modes of the $[–N(CH_3)_3]^+$ polar head group were not observed due to their interaction with the silica walls and to the presence of structural water molecules [42]. After $HDTMA^+$ removal, these bands red shifted to 2921 and 2850 cm^{-1} respectively and a new band appeared at 2956 cm^{-1}. Band shifting to lower frequencies correspond to an increasing of the *trans* conformer that presents a more ordered liquid crystalline state than the *gauche* conformer [41, 42]. This phenomenon is normally observed when $HDTMA^+$ micelles, with less structural ordering, go through a phase transition to a crystalline phase, with an all *trans* conformation of methylene groups [40, 42]. Improvement on the structural ordering after $HDTMA^+$ removal was also observed in the registered X-ray diffraction patterns (Fig. 1) and might be related to the presence of less mobile C_{16}-chains due to the covalent bond with the silica wall. The new band at 2956 cm^{-1} was assigned to the C–H asymmetrical stretching of terminal methyl groups of the C_{16}-chains, that became freely to rotate when $HDTMA^+$ molecules were absent [41].

Ibuprofen loading into C_{16}MCM-41 was confirmed by the observation of characteristics bands of the molecule at 1711 and 1514 cm^{-1} in FTIR spectra (Fig. 3b), respectively attributed to the stretching of the carboxylic acid group and to the C=C of the aromatic ring. Shifts in frequencies of C–H stretching modes of alkyl chains were not observed after ibuprofen immobilization, which suggests a poor interaction of drug molecules with the pendants C_{16}-chains. Thus, the drug molecules should be positioned near the silica walls, with the polar portion interacting to terminal silanol groups. That arrangement is compatible to the one that was reported to ibuprofen loaded MCM-41 [32], where a shift to a lower frequency of the C=O stretching mode, when compared to the frequency observed to ibuprofen in solid state, was attributed to this interaction. Ibuprofen in solid state has a crystalline structure composed of hydrogen bonded dimers [43], where the C=O stretching mode of the carboxylic acid group is observed at 1721 cm^{-1} (see Figure S3 in Electronic Supplementary Material). In the FTIR spectrum of Ibu@C_{16}MCM-41 (Fig. 3b) this band was observed at 1711 cm^{-1} indicating a weakening of the C=O bond.

Vibrational bands around 1628 cm^{-1} in the FTIR spectra (Fig. 3b) were attributed to O–H bending of residual water molecules retained in silica framework and bands at around 1470 cm^{-1} were attributed to out-of-plane bending of C–H bond. Significant frequency changes were observed after $HDTMA^+$ removal, when bands around 1468 cm^{-1} became narrow and intense, which is in agreement to the proposed increasing of *trans* conformer.

At 1400–400 cm^{-1} range the vibrational spectra are dominated by the intense bands of the silica framework [35] that are superimposed to some bending vibrational modes of C_{16}-chains and ibuprofen molecules. Thus, this spectral region was not useful to get information about the molecular packaging and organization (see Figure S3 in Electronic Supplementary Material).

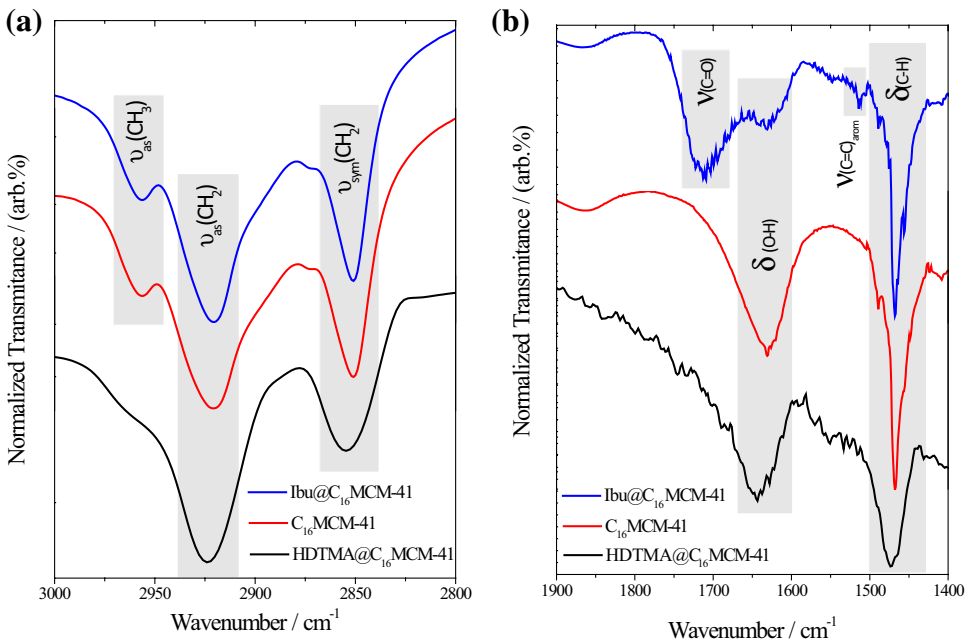

Fig. 3 Selected regions of the FTIR spectra of silicas mesostructures. **a** Spectral range dominated by stretching modes of C–H bond in C_{16}-chains. **b** Spectral range dominated by vibrational bands of ibuprofen and C–H bending of C_{16}-chains

3.2 Ibuprofen release properties

At first a calibration curve of ibuprofen absorption at 263 nm in SBF using solutions of known molar concentrations was created in order to determine the molar absorption coefficient necessary to calculate the cumulative amount of drug released along the time. Calculated linear equation was $A = 0.008 + 335.7\ C$ with a R^2 of 0.996 (see Figure S4 in Electronic Supplementary Material).

The ibuprofen release from C_{16}MCM-41 (Fig. 4a) occurred at a rate slower than the one observed for MCM-41 and propylamine-grafted MCM-41 (MCM-41NH_2) (see Figure S5 in Electronic Supplementary Material). Despite of similarity of the ibuprofen release rates from C_{16}MCM-41 and MCM-41NH_2, the chemical interaction involved in both mesostructures are quite different. Ibuprofen molecules loaded into MCM-41NH_2 interact strongly to the inorganic framework, since the grafted amine groups subtract protons of the carboxylic acid group of ibuprofen molecule promoting a coulomb interaction [37]. On the other hand, the drug interaction to the mesostructure in C_{16}MCM-41 and MCM-41 are very similar, but the release rates are quite different. Thus, to achieve a better understand of the ibuprofen release phenomenon the Korsmeyer-Peppas kinetic model [44], which is a more comprehensive model than the Higuchi normally adopted [45], was applied to the experimental cumulative drug release curve (Fig. 4a). By plotting the Korsmeyer-Peppas linear equation using the experimental data (Fig. 4b) the values of k (rate constant) and n (release exponent) were calculated. The rate constant k incorporates the influence and characteristics of the silica particles and the exponent n is related to the diffusion mechanism. When n value is lower than 0.5, the release is a Fickian's diffusion process that matches the Higuchi model. If n is between 0.5 and 1.0, the diffusion is anomalous and if n is equal to 1, the release obeys a zero-order kinetic [45].

The kinetics of ibuprofen release from MCM-41 or MCM-41NH_2 silicas normally matches the Higuchi model (see Figure S6 in Electronic Supplementary Material), but in the case of C_{16}MCM-41 the calculated release exponent (n) of 0.74 indicates the presence of an anomalous transport, that might be related to a contribution of diffusional (drug and solvent) and relaxational (C_{16}-chain) components to the release process, as observed in polymeric drug carriers. The calculated rate constant (k) was 0.048 h^{-1}, which confirmed a slower rate of ibuprofen release in C_{16}MCM-41 compared to MCM-41 and MCM-41NH_2 (see Figure S6 in Electronic Supplementary Material).

4 Conclusions

This study showed the production of a hydrophobic hexagonal silica mesostructure containing mesopores filled with hexadecyl chains grafted into the silica walls. A p6mm mesostructure with a long range ordering was obtained by a modified direct synthesis procedure where half of the structure directing agent molar amount required to producing the hexagonal mesophase was replaced by hexadecyltrimethoxysilane. C_{16}-chains located inside the pores made the silica non porous and highly hydrophobic but preserved the capability of retention drug molecules into the voids of alkylic chains. Hydrophobic interactions influenced the ibuprofen release kinetics in SBF. The drug release from C_{16}MCM-41 was slower than the ones observed for MCM-41 and MCM-41NH_2 and the process was influenced by an anomalous transport phenomenon with contribution of diffusional and relaxational components, similar to what is observed to swellable polymeric drug delivery systems. The produced hydrophobic mesostructure has the potential use as a carrier for low water soluble drugs with an extended delivery effect, but without the disadvantages of co-releasing toxic surfactant molecules or the need of non-toxic specific templates to be prepared.

Acknowledgements Authors are thankful to Prof. Vera R. L. Constantino (IQ-USP) and Ricardo Couto (IQ-USP) for the support on X-ray diffractometry and thermogravimetric experiments. M. A. Bizeto is thankful to the financial support from Fundação de Amparo à Pesquisa do Estado de São Paulo (FAPESP) (Grant 2011/50318-1). M. B. Costa is thankful to Coordenação de Aperfeiçoamento de Pessoal de Nível Superior (CAPES) for the research fellowship.

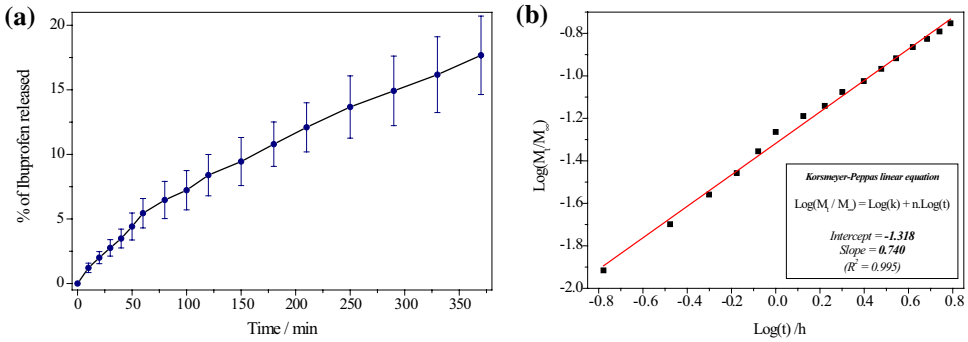

Fig. 4 **a** Cumulative curve of ibuprofen release from C_{16}MCM-41 in SBF (pH 7.4). **b** Plot of the Korsmeyer-Peppas linear equation where M_t is the amount of ibuprofen released at the time t, M_∞ is the ibuprofen amount in the carrier (expected to be released as time proceeds to infinity), k is the kinetic rate constant and n is the Korsmeyer-Peppas exponent

References

1. V. Meynen, P. Cool, E.F. Vansant, Microporous Mesoporous Mater. **125**, 170 (2009)
2. Z. Li, J.C. Barnes, A. Bosoy, J.F. Stoddart, J.I. Zink, Chem. Soc. Rev. **41**, 2590 (2012)
3. P. Yang, S. Gai, J. Lin, Chem. Soc. Rev. **41**, 3679 (2012)
4. A. Walcarius, L. Mercier, J. Mater. Chem. **20**, 4478 (2010)
5. L.T. Gibson, Chem. Soc. Rev. **43**, 5163 (2014)
6. L.T. Gibson, Chem. Soc. Rev. **43**, 5173 (2014)
7. A. Corma, H. Garcia, Adv. Synth. Catal. **348**, 1391 (2006)
8. M.P. Conley, C. Copéret, C. Thieuleux, ACS Catal. **4**, 1458 (2014)
9. S. Rostamnia, E. Doustkhah, RSC Adv. **4**, 28238 (2014)
10. J. Zhu, Y. Niu, Y. Li, Y. Gong, huihui Shi, Y. Liu, Q. Xu, Q.Q. Huo, Y. Liu, Q. Xu, J. Mater. Chem. B **5**, 1339 (2017)
11. K. Moller, T. Bein, Chem. Mater. **10**, 2950 (1998)
12. A. Stein, B.J. Melde, R.C. Schroden, Adv. Mater. **12**, 1403 (2000)
13. M.H. Lim, A. Stein, Chem. Mater. **11**, 3285 (1999)
14. A. Walcarius, C. Delacôte, Chem. Mater. **15**, 4181 (2003)
15. N. Baccile, F. Babonneau, Microporous Mesoporous Mater. **110**, 534 (2008)
16. N.A. Vodolazkaya, C. Despas, B. Lebeau, C. Marichal, A. Walcarius, J. Sol-Gel Sci. Technol. **63**, 587 (2012)
17. C. Huo, M. Li, X. Huang, H. Yang, S. Mann, Langmuir **30**, 15047 (2014)
18. J.S. Valenstein, K. Kandel, F. Melcher, I.I. Slowing, V.S.-Y. Lin, B.G. Trewyn, ACS Appl. Mater. Interfaces **4**, 1003 (2012)
19. F. Quan, Y. Hu, X. Liu, C. Wei, Phys. Chem. Chem. Phys. **17**, 19401 (2015)
20. B. Zou, Y. Hu, F. Cui, L. Jiang, D. Yu, H. Huang, J. Colloid Interface Sci. **417**, 210 (2014)
21. Q. Tang, Y. Xu, D. Wu, Y. Sun, Chem. Lett. **35**, 474 (2006)
22. Q. Tang, Y. Xu, D. Wu, Y. Sun, J. Wang, J. Xu, F. Deng, J. Control. Release **114**, 41 (2006)
23. Q. Tang, Y. Chen, J. Chen, J. Li, Y. Xu, D. Wu, Y. Sun, J. Solid State Chem. **183**, 76 (2010)
24. N.W. Clifford, K.S. Iyer, C.L. Raston, J. Mater. Chem. **18**, 162 (2008)
25. N. Vlachy, D. Touraud, J. Heilmann, W. Kunz, Colloids Surf B **70**, 278 (2009)
26. C.-H. Tsai, J.L. Vivero-Escoto, I.I. Slowing, I.-J. Fang, B.G. Trewyn, V.S.-Y. Lin, Biomaterials **32**, 6234 (2011)
27. P. Botella, A. Corma, M. Quesada, J. Mater. Chem. **22**, 6394 (2012)
28. T. Kokubo, H. Takadama, Biomaterials **27**, 2907 (2006)
29. J.S. Beck, J.C. Vartuli, W.J. Roth, M.E. Leonowicz, C.T. Kresge, K.D. Schmitt, C.T.W. Chu, D.H. Olson, E.W. Sheppard, S.B. McCullen, J.B. Higgins, J.L. Schlenker, J. Am. Chem. Soc. **114**, 10834 (1992)
30. F. Mariano-Neto, J.R. Matos, L.C. Cides da Silva, L.V. Carvalho, K. Scaramuzzi, O.A. Sant'Anna, C.P. Oliveira, M.C.A. Fantini, J. Phys. D **47**, 425402 (2014)
31. C. Charnay, S. Bégu, C. Tourné-Péteilh, L. Nicole, D.A.A. Lerner, J.M.M. Devoisselle, Eur. J. Pharm. Biopharm. **57**, 533 (2004)
32. T. Azaïs, C. Tourné-Péteilh, F. Aussenac, N. Baccile, C. Coelho, J.-M. Devoisselle, F. Babonneau, Chem. Mater. **18**, 6382 (2006)
33. K.S.W. Sing, D.H. Everett, R.A.W. Haul, L. Moscou, R.A. Pierotti, J. Rouquerol, T. Siemieniewska, Pure Appl. Chem. **57**, 603–619 (1985).
34. M. Thommes, K. Kaneko, A.V. Neimark, J.P. Olivier, F. Rodriguez-Reinoso, J. Rouquerol, K.S.W. Sing, Pure Appl. Chem. **87**, 1051 (2015)
35. L.C. Fonseca, R. Faez, F.F. Camilo, M.A. Bizeto, Microporous Mesoporous Mater. **159**, 24 (2012)
36. M. Vallet-Regi, A. Rámila, R.P. del Real, J. Pérez-Pariente, Chem. Mater. **13**, 308 (2001)
37. B. Muñoz, A. Rámila, J. Pérez-Pariente, I. Díaz, M. Vallet-Regí, Chem. Mater. **15**, 500 (2003)
38. R.A. MacPhail, H.L. Strauss, R.G. Snyder, C.A. Elliger, J. Phys. Chem. **88**, 334 (1984)
39. R.G. Snyder, H.L. Strauss, C.A. Elliger, J. Phys. Chem. **86**, 5145 (1982)
40. N.V. Venkataraman, S. Vasudevan, J. Phys. Chem. B. **104**, 11179 (2000)
41. W. Wang, L. Li, S. Xi, J. Colloid Interface Sci. **155**, 369 (1993)
42. K.H.S. Kung, K.F. Hayes, Langmuir **9**, 263 (1993)
43. A.A. Freer, J.M. Bunyan, N. Shankland, D.B. Sheen, Acta Crystallogr. Sect. C **49**, 1378 (1993)
44. R.W. Korsmeyer, R. Gurny, E. Doelker, P. Buri, N.A. Peppas, Int. J. Pharm. **15**, 25 (1983)
45. J. Siepmann, N.A. Peppas, Int. J. Pharm. **418**, 6 (2011)